HHS Public Access

Author manuscript

J Orthop Res. Author manuscript; available in PMC 2019 January 24.

Published in final edited form as:

J Orthop Res. 2016 April ; 34(4): 641–649. doi:10.1002/jor.23066.

Indian Hedgehog Signaling and the Role of Graft Tension in Tendon-to-Bone Healing: Evaluation in a Rat ACL Reconstruction Model

Andrew Carbone[1], **Camila Carballo**[1], **Richard Ma**[2], **Hongsheng Wang**[1], **Xianghua Deng**[1], **Chitra Dahia**[1], and **Scott Rodeo**[1]

[1]Hospital for Special Surgery, 535 E. 70th Street, New York 10021, New York

[2]Missouri Orthopaedic Institute, University of Missouri, Columbia, Missouri

Abstract

The structure and composition of the native enthesis is not recapitulated following tendon-to-bone repair. Indian Hedgehog (IHH) signaling has recently been shown to be important in enthesis development in a mouse model but no studies have evaluated IHH signaling in a healing model. Fourteen adult male rats underwent ACL reconstruction using a flexor tendon graft. Rats were assigned to two groups based on whether or not they received 0N or 10N of pre-tension of the graft. Specimens were evaluated at 3 and 6 weeks post-operatively using immunohistochemistry for three different protein markers of IHH signaling. Quantitative analysis of staining area and intensity using custom software demonstrated that IHH signaling was active in interface tissue formed at the healing tendon-bone interface. We also found increased staining area and intensity of IHH signaling proteins at 3 weeks in animals that received a pre-tensioned tendon graft. No significant differences were seen between the 3-week and 6-week time points. Our data suggests that the IHH signaling pathway is active during the tendon-bone healing process and appears to be mechanosensitive, as pre-tensioning of the graft at the time of surgery resulted in increased IHH signaling at three weeks.

Keywords

tendon-bone healing; Indian hedgehog; PTCH1; GLI1; ACL reconstruction

Reconstruction of the anterior cruciate ligament (ACL) using a tendon graft is a commonly performed surgical procedure. Soft tissue autografts (such as semitendonosis and/or gracilis) or allografts (such as semitendonosis, tibialis tendon) require secure healing between the tendon and the bone tunnel. Anterior cruciate ligament graft function is dependent upon secure healing of the tendon graft in the bone tunnels. Repeated cyclical loading leads to an element of graft-tunnel motion, which may impair or delay healing and lead to recurrent

Correspondence to: Scott Rodeo (T: 1-212-606-1513; F: 1-212- 774-2414; rodeos@hss.edu).

AUTHORS' CONTRIBUTIONS

A.C., C.C., C.D., S.R., conceived and designed the study. R.M. and X.D. were responsible for performing the surgical procedures. A.C., H.W., and C.C were responsible for collection of data. A.C., C.C., C.D. and S.R. were responsible for data analysis and writing of the article.

joint laxity. Excessive strain loading of an ACL graft can result in lengthening of the bone-graft-bone construct; the majority of that lengthening occurs in the bone tunnels (not in the joint cavity) and can result in an increase in anterior knee laxity and affect the stability of the reconstructed knee, which may result in knee instability, poor patient satisfaction and ultimately, graft failure.[1]

Numerous factors affect healing between soft tissue and bone, including biologic (cytokines, pluripotent cells, etc.) and mechanical factors. Previous studies demonstrate that the complex structure and composition of the native enthesis tissue connecting tendon to bone is not regenerated.[2] Instead of formation of the mineralized fibrocartilage zone of the native tendon (or ligament) enthesis, a fibrovascular scar tissue interface forms at the healing attachment site. This scar tissue lacks the biomechanical properties of the native enthesis tissue.[3] Understanding the cellular and molecular mechanisms involved in mechanotransduction at the healing tendon-bone interface can ultimately provide insights into ways to improve graft-to-bone healing.

Our laboratory has been investigating the effect of mechanical load on healing of a tendon graft in a bone tunnel.[4–6] The mechanical environment at the healing tendon-bone interface is affected by several different variables, including the amount of initial graft tension, the position of the bone tunnels, physical properties of the graft, and positioning of the knee at time of fixation.[7–10] The optimal level of initial graft tension and its effect on the biologic events of healing is unknown.[11] Excessive graft tension may adversely affect graft revascularization and remodeling.[12] It is also known that excess initial tension can cause deterioration of the graft-bone connective tissue interface.[13] On the other hand, lack of graft tension leads to stress deprivation of the graft and resultant matrix degradation due to matrix metalloproteinase expression.[14]

Indian hedgehog (IHH) is a signaling protein in the hedgehog (Hh) family, which has recently drawn interest for its role in tendon-bone development.[15–17] IHH signaling by chondrocytes has been shown to be stimulated by mechanical strain in vitro.[18–20] IHH expression has also been shown to be responsible for stimulatory effects on chondrocyte proliferation, differentiation and repair.[18,20–24] Furthermore, recent studies in transgenic embryonic mouse models have linked IHH signaling to the development of the fibrocartilagenous attachment tissue at the tibial insertion site of the patellar tendon.[15] In addition, IHH signaling knockout mice demonstrate significant histological, biomechanical, and gene expression changes at tendon insertion sites when compared to age-matched controls.[25]

No studies have evaluated IHH signaling during tendon-to-bone healing in the post-natal animal. Thus, the purpose of our study was to test the hypothesis that the IHH signaling pathway is active at the graft-bone interface during the healing process in a rat ACL reconstruction model. Furthermore, we evaluated the effect of initial graft tension on IHH signaling. To our knowledge, this is the first study to quantitatively evaluate IHH signaling and its effect on healing in an ACL reconstruction model. We used immunohistochemical staining to examine the spatial and temporal expression of IHH and two downstream

proteins in the IHH signaling cascade, Patched 1 (PTCH1) and GLI1, which are up-regulated by IHH signaling activity.[26]

METHODS

Overview

All aspects of the experiments were approved by our Institutional Animal Care and Use Committee (IACUC). Rats used in study were 12-week-old male Sprague Dawley rats weighing between 300–350 g. Rats used for our positive control growth plate staining were 6-week-old Sprague Dawley rats weighing between 125–150 g. Using surgical techniques developed during a previous study, we carried out ACL reconstruction using an autograft taken from the flexor digitorum longus tendon. The animals were divided into two groups: (i) ACL graft fixed with no tension (0N) and (ii) ACL graft fixed under 10N of tension intraoperatively. An external fixator was placed on the operative knee to eliminate post-operative joint motion and resultant ACL graft load. The rats were then allowed to return to normal cage activity. Seven rats were sacrificed at 3 weeks (3 rats with 0N pretension, 4 rats with 10N pretension) and the remaining rats were sacrificed at 6 weeks post-operatively (4 rats with 0N pretension, 3 rats with 10N of pretension). These time points correspond to a previous study which showed significant differences between high and low graft pre-tension in a similar rat ACL reconstruction model prior to 6 weeks.[27] Following sacrifice, the tissues were prepared for immunohistochemistry (IHC). Images were analyzed independently by two observers using custom software (MATLAB, MathWorks Inc., Natick, MA) designed to quantify staining using a color matching algorithm.

ACL Reconstruction

All 14 rats underwent right knee ACL reconstruction using a soft tissue autograft. The flexor digitorum longus (FDL) tendon autograft was harvested from the ipsilateral limb through small incisions on the posteromedial ankle and plantar foot. The FDL tendon was then prepared with a 4–0 Ethibond locking Krackow stitch (Ethicon, Somerville, NJ) placed on each end of the tendon autograft. Once the autograft was harvested, the knee was then exposed via a medial parapatellar arthrotomy. Following the arthrotomy, the patella was translated laterally, which provided the exposure to the intercondylar notch of the knee. The ACL was then identified under loupe magnification and fully sectioned using a #11 surgical blade. Once the ACL was transected, the femoral and tibial bone tunnels were drilled using a 1.4 mm k-wire. Care was taken to create the bone tunnels in a consistent location in all animals, entering the joint at the ACL tibial footprint. The FDL tendon autograft was then shuttled through both the tibial and femoral tunnels using the attached 4–0 sutures. The femoral side was fixed first by passing a 3–0 surgical steel suture wire (Ethicon, Somerville, NJ) through a transverse drill hole in the femoral metaphysis just above the tunnel exit. This wire was then looped tightly around the graft adjacent to the exit from the femoral tunnel. The knee was then brought to 30° of flexion and the graft was fixed on the tibial side with a wire that had been passed through a drill hole at the level of the tibial tuberosity similar to the femoral side after either 0N or 10N pre-tensioning. One 0.9 mm threaded pin was then placed into the femoral shaft and two 0.9 mm threaded pins into the tibial shaft, and a

custom-designed metal external fixator was attached to the pins to immobilize the knee at 90˚ of flexion to eliminate joint motion and further ACL graft loading.

Tensioning of the Graft

The animals were allocated to a static pretension load of 0N (non-tensioned) or 10N (over-tensioned). For the 10N group, the graft was first fixed on the femoral side, and then a suture attached to the tibial end of the graft was attached to a one kilogram free weight via a pulley system in order to achieve 10N pretension force with the knee at 30˚ flexion. The wire was then rigidly tightened over the graft at the tibial tunnel exit. For the 0N group, a 0N-pretensioned graft was simply passed and secured in situ without any tension applied to either end of the graft during fixation.

Histological Analysis

Rats were sacrificed using CO_2 asphyxiation at 3 and 6 weeks post-surgery. Rat hindlimbs were removed and fixed in 10% formalin solution followed by decalcification for 3 days (Immunocal, Decal Chemical Corp, Tallman, NY). The tissues were then trimmed, embedded in paraffin wax, and serial 4 mm sections were made using a microtome. Following sectioning, 4 mm specimens were placed on slides and serial sections were blocked with 1% serum for 10 min at room temperature; antigen retrieval was performed incubating sections in trypsin for 15 min at 37˚C, Next, sections were incubated with each of the primary antibodies (IHH-1:500 Ab52919, Abcam Cambridge, MA; PTCH-1:1,000 Ab53715, Abcam Cambridge, MA; GLI 1–1:500 Ab151796, Abcam Cambridge, MA; PCNA-1:400 13–3,900, Life Technologies Grand Island, NY) for 1 h at room temperature An undiluted LSAB2 system-HRP was used (LSAB2 System-HRP K0609 Dako Carpinteria, CA). Finally, Liquid DAB + Substrate Chromogen system (Dako K3468 Carpinteria, CA) was applied. Negative controls were performed in exactly the same fashion with the exception of the primary antibody.

Imaging

All slides were imaged using a Nikon Eclipse Ni-E (Nikon Instruments Melville, NY). Images were taken at 10× magnification, and the entire graft-bone interface for each rat specimen was imaged.

Image Quantification

Using commercially available Adobe Photoshop software (Adobe Corporation), all images were compiled together using the “photomerge” function and a composite image of each sample was created for all three antibody stains as well as the negative control such that the entire tendon bone interface could be visualized on one image. Next, 5 Red Green Blue (RGB) values corresponding to true positive staining were identified for each specimen stained against IHH. Values were averaged to determine one RGB value which was input into the computer to be used to analyze all three stains as well as the negative control for each specimen. Two independent and blinded observers then isolated the entire tendon bone interface from the composite image. These composite images containing the entire isolated tendon-bone interface from each rat specimen and each immunohistochemical stain were

then input into our software along with RGB values corresponding to true positive staining. The software performed a quantitative evaluation of the images from each of the observers according to a color matching algorithm and results were averaged. The program calculated area in pixels as well as the intensity of the IHC staining. These values were standardized against the total area in pixels of each composite image in order to normalize for comparison. Representative sample images demonst rating our image analysis technique can be seen in Figure 1.

Statistical Analysis

Kruskal–Wallis one-way analysis of variance (Statistics Toolbox, MATLAB, MathWorks, Natick, MA) was used to compare the immunohistochemical staining data between pretension groups and different post-operative time points. Significance was set at $p < 0.05$.

RESULTS

Histologic Analysis

A low power H&E image is shown in Figure 2 which demonstrates the orientation of the tendon graft in the tibial tunnel. Only bone-graft interfaces from the tibial tunnel were analyzed. Qualitative analysis of all three stains demonstrated that IHH signaling is active in interface tissue formed at the healing tendon-bone interface. Figure 3 shows staining of an age-matched native rat ACL enthesis for IHH signaling proteins for comparison. Staining was not uniformly distributed along the tendon-bone interface. There tended to be increased tissue organization, more complete graft integration into the surrounding bone, and a wider and more regularly shaped graft-bone interface on one side of the graft-bone interface than the other. More cells staining positive for IHH signaling were located in areas where there was a more organized graft-bone interface. A representative image demonstrating differences between the two sides can be seen in Figure 4. There were some areas in the bone tunnel where the tendon appeared to have very little contact with the adjacent bone. In these areas, there tended to be a narrower, more irregular adjacent bone interface with less staining for hedgehog proteins. Figure 5 demonstrates a representative image from a negative control section compared to the same area of tendon-bone interface on a serial section from the same rat stained against PTCH1.

Quantitative Histologic Analysis

IHH Signaling—Computerized image analysis confirmed that IHH signaling is active at the tendon-bone interface, with positive staining demonstrated for all markers (GLI1, PTCH1, and IHH) (Fig. 6). A list of all raw data along with standard deviations can be seen in Table 1. One sample from the negative control group was eliminated due to improper antibody exposure time.

0N versus 10N Graft Pre-Tension—Significant differences were seen between the 0N and 10N groups at 3 weeks in terms of the area of the graft-bone interface stained. Specifically, differences were seen in PTCH1 ($p < 0.04$) and GLI1 ($p < 0.04$) which showed increased staining in rats whose grafts were fixed under 10N of tension as compared to those whose grafts were fixed with 0N of tension (Fig. 5). There were also statistically significant

differences in staining intensity for PTCH1 ($p < .04$) and GLI1 ($p < .04$), with greater staining in the 10N group at 3 weeks (Fig. 5). There were no significant differences between 0N and 10N groups in area of the graft-bone interface stained or staining intensity for PTCH1 and GLI1 at 6 weeks (Fig. 5). There were no statistically significant differences in IHH protein staining between any of the experimental groups (3 week 0N vs 10N, $p = 0.64$; 6 week 0N vs. 10N, $p = 0.64$).

Three-vs. Six-Weeks—No statistically significant differences were seen between the 3 and 6 week time points when controlling for initial graft tension. However, when comparing the 0N group between 3 weeks and 6 weeks, we found that there was a trend toward increased intensity and area of staining in the 6 week 0N group compared to the 3 week 0N group for both PTCH ($p = 0.114$) and GLI1 ($p = 0.057$). This trend was not seen when comparing the 10N groups across time. Raw data can be seen in Table 1.

PCNA Staining—PCNA staining performed on 3 and 6 week samples demonstrates active cellular proliferation at the tendon-bone interface. This staining appeared to be more intense in our 3 week group than our 6 week group. There also appeared to be proliferation occurring in the tendon mid-substance, albeit to a much lesser extent than that occurring at the tendon-bone interface. Representative images from our 3 and 6 week samples are seen in Figure 7 as well as control from the articular cartilage of a 6 week old rat femur.

DISCUSSION

Our data suggests that the IHH pathway is active during the tendon-bone healing process. While a role for IHH signaling has been reported in insertion site formation in the developing embryo, no studies have examined its role during post-natal healing. Given the role of IHH signaling in bone and cartilage formation, it is reasonable to conclude that this factor plays an important role in insertion site healing. The positive localization of IHH as well as PTCH1 and GLI1 (two downstream proteins in the IHH signaling cascade) provides strong evidence that IHH plays a role in tendon-to-bone healing.

The stimulation of chondrocyte proliferation and mineralization appears to be a necessary step in the regeneration of native fibrocartilagenous enthesis tissue, which consists of two layers of fibrocartilage between tendon and bone, one mineralized and one nonmineralized.[28] Previous studies have shown that IHH expression is partially regulated by mechanical stretch, with increasing strain demonstrating higher levels of chondrocyte proliferation.[18–20,29,30] Our findings also suggest that mechanical load at the healing interface may affect IHH signaling as there was increased IHH signaling with higher initial graft tension. However, these effects were lost by the 6-week time point, suggesting that whatever role graft tension plays in IHH signaling may only be demonstrated early in the repair process. This finding is similar to a recent study in a rat ACL reconstruction model that showed that pre-tensioning of the ACL graft at 5% and 10% (2N and 4N) of ultimate graft strength resulted in significantly increased graft ultimate failure load at 2 weeks in addition to showing decreased joint laxity.[27] The 10% group demonstrated significantly better results in both categories compared to the 5% group.[27] Histologically, the 10% group also demonstrated enhanced graft incorporation into the bone tunnel. Similar to our findings,

these differences between the 5% and 10% groups were not seen at the 6-week time point. We hypothesize that initial mechanical strain on the ACL graft results in up-regulation of the IHH signaling pathway, and that this increased activity could be partially responsible for improvements in the biologic healing process.

Further support for a potential effect of mechanical loading on IHH signaling comes from the finding that the amount of positive immunostaining was higher in areas with greater tendon-bone contact and a more organized tissue interface. We believe that the difference in the morphology of the healing interface on one side of the tunnel versus the other is due to different mechanical environments. Knee motion likely leads to a complex loading environment, with tension, compression, and shear on the graft-bone tunnel interface. Further study is required to understand how mechanical factors at the healing graft-bone interface affect important signaling mechanisms.

PCNA staining demonstrated enhanced cellular proliferation at the tendon-bone interface. Areas of enhanced cellular proliferation were consistent with the same areas which demonstrated high levels of IHH signaling. This finding is compatible with previous literature which has shown IHH signaling to be responsible for the stimulation of chondrocyte proliferation, differentiation, and mineralization,[18,21–24,31–34] and crucial for the proper development of mature tendon-bone attachment tissue.[25]

We were also able to appreciate a small but noticeable qualitative difference in PCNA staining between our 3 and 6 week groups, with our 3 week group demonstrating slightly more PCNA staining than the 6 week animals. Our data demonstrates that IHH signaling is persistently active 6 weeks post-ACL reconstruction at or above levels seen in our 3 week groups. We hypothesize that the role of IHH signaling in the tissue repair process is more complex than as a simple growth factor. It is possible that through the interactions with other related pathways, IHH signaling's role in the repair process may change depending on the concentration of different cytokines in the surrounding microenvironment. It appears likely that IHH signaling alone is insufficient to maintain cellular proliferation, but that it may interact with other growth factors early in the healing process to stimulate cellular proliferation at the interface. In later stages of repair, IHH signaling may interact with different growth factors to direct other cellular processes such as mineralization of the chondrocyte-like cells. Further study analyzing the temporal expression of relevant growth factors at the tendon-bone interface, as well as analyzing the repair process in IHH signaling knock-out animals are needed. Such studies would help to explain why even though cellular proliferation of chondrocyte-like cells is occurring along with the activation of pathways responsible for chondrocyte mineralization, regeneration of the highly organized mineralized fibrocartilagenous layer of attachment tissue, seen in the native fibrocartilaginous entheses, still does not occur.

Improving the strength of the tissue connecting the graft to the bone tunnel may help to improve the biomechanical performance of the graft by minimizing graft lengthening, micro-motion, and joint laxity. By understanding the potential relationship between IHH signaling and its effects on graft-bone healing, we may be able to optimize the healing response and improve patient outcomes.

An important limitation of this study is the relatively small number of animals that were evaluated ($n = 14$). However, robust and specific immunostaining with all three markers verifies the activity of the IHH signaling pathway. Examination of both earlier and later time points will shed further light on the spatial and temporal aspects of IHH signaling. Further studies may use biomechanical testing to correlate IHH signaling with structural and material properties of the healing insertion site. Lastly, given the possibility that IHH signaling is affected by biomechanical loading, control of post-operative knee motion and animal activity will provide insight into how IHH activity is affected by mechanical load, which would have implications for post-operative rehabilitation protocols in patients.

In conclusion, this study is the first to demonstrate that IHH signaling is active during tendon-bone healing in an adult animal model, and suggests that biomechanical stress on the healing tissue affects signaling. In addition we have shown that there is a spatial relationship between areas of cellular proliferation and IHH signaling as demonstrated by PCNA staining. Since the IHH pathway plays an important role in bone, cartilage, and enthesis formation in embryogenesis, it is plausible that this signaling pathway plays an important role in those tissues during repair as well. The translational aspect of this work lies in the identification of factors that may eventually serve as therapeutic targets for intervention.

ACKNOWLEDGMENTS

We would like to thank Lilly Ying for the histology work. This study was funded by a grant from the Orthopaedic Research and Education Foundation and the Virginia Toulmin Foundation. S.A.R. is a consultant for Rotation Medical, Inc., Pluristem Therapeutics, Inc., and Cytori Therapeutics, Inc., and has stock in Cayenne Medical.

Grant sponsor: Orthopaedic Research and Education Foundation;

Grant sponsor: Virginia Toulmin Foundation.

REFERENCES

1. Roos P, Hull M, Howell S. 2004 Lengthening of double-looped tendon graft constructs in three regions after cyclic loading: a study using roentgen stereophotogrammetric analysis. J Orthop Res 22:839–846. [cited 2014 Nov 30] Available from: Http://onlinelibrary.wiley.com/doi/10.1016/j.orthres.2003.11.002/abstract [PubMed: 15183443]
2. Rodeo SA, Arnoczky SP, Torzilli PA, et al. 1993 Tendon-healing in a bone tunnel. A biomechanical and histological study in the dog. Joint Bone J Surg 75:1795–1803.
3. Chan BP, Fu SC, Qin L, et al. 1998 Pyridinoline in relation to ultimate stress of the patellar tendon during healing: an animal study. J Orthop Res 16:597–603. Available from http://www.ncbi.nlm.nih.gov/pubmed/9820284 [PubMed: 9820284]
4. Packer JD, Bedi A, Fox AJ, et al. 2014 Effect of immediate and delayed high-strain loading on tendon-to-bone healing after anterior cruciate ligament reconstruction. J Bone Joint Surg Am 96:770–777. Available from: http://www.ncbi.nlm.nih.gov/pubmed/24806014 [PubMed: 24806014]
5. Bedi A, Kovacevic D, Fox AJS, et al. 2010 Effect of early and delayed mechanical loading on tendon-to-bone healing after anterior cruciate ligament reconstruction. J Bone Joint Surg Am 92:2387–2401. [cited 2014 Oct 20] Available from: http://www.pubmedcentral.nih.gov/articlerender.fcgi?artid=2947356&tool=pmcentrez&rendertype=abstract [PubMed: 20962189]
6. Brophy RH, Kovacevic D, Imhauser CW, et al. 2011 Effect of short-duration low-magnitude cyclic loading versus immobilization on tendon-bone healing after ACL reconstruction in a rat model. J Bone Joint Surg Am 93:381–393. [PubMed: 21325590]
7. Suggs J, Wang C, Li G. 2003 The effect of graft stiffness on knee joint biomechanics after ACL reconstruction—a 3D computational simulation. Clin Biomech 18:35–43.

8. Bylski-Austrow D, Grood E. 1990 Anterior cruciate ligament replacements: a mechanical study of femoral attachment location, flexion angle at tensioning, and initial tension. J Orthop Res 8:522–531. [cited 2014 Dec1] Available from: http://www.ncbi.nlm.nih.gov/pubmed/2355292 [PubMed: 2355292]

9. Fleming B, Beynnon B. 1992 Effect of tension and placement of a prosthetic anterior cruciate ligament on the anteroposterior laxity of the knee. J Orthop Res 10:177–186. [cited 2014 Nov 23] Available from: http://www.ncbi.nlm.nih.gov/pubmed/1740735 [PubMed: 1740735]

10. Sherman SL, Chalmers PN, Yanke AB, et al. 2012 Graft tensioning during knee ligament reconstruction: principles and practice abstract. J Am Acad Orthop Surg 20:633–645. [PubMed: 23027693]

11. Nicholas SJ. 2004 A prospectively randomized double-blind study on the effect of initial graft tension on knee stability after anterior cruciate ligament reconstruction. Am J Sports Med 32:1881–1886. [cited 2014 Nov 24] Available from: http://journal.ajsm.org/cgi/doi/10.1177/0363546504265924 [PubMed: 15572316]

12. Peña E, Mart´nez a M, Calvo B, et al. 2005 A finite element simulation of the effect of graft stiffness and graft tensioning in ACL reconstruction. Clin Biomech (Bristol Avon) 20:636–644. [cited 2014 Nov 23] Available from: http://www.ncbi.nlm.nih.gov/pubmed/15927737

13. Katsuragi R, Yasuda K, Tsujino J. 2000 The effect of nonphysiologically high initial tension on the mechanical properties of in situ frozen anterior cruciate ligament in a canine model. Am J Sports Med 28:47–56. [cited 2014 Dec 2] Available from: http://ajs.sagepub.com/content/28/1/47.short [PubMed: 10653543]

14. Arnoczky SP, Lavagnino M, Egerbacher M, et al. 2007 Matrix metalloproteinase inhibitors prevent a decrease in the mechanical properties of stress-deprived tendons: an in vitro experimental study. Am J Sports Med 35:763–769. [cited 2014 Dec 15] Available from: http://www.ncbi.nlm.nih.gov/pubmed/17293464 [PubMed: 17293464]

15. Liu C-F, Aschbacher-Smith L, Barthelery NJ, et al. 2012 Spatial and temporal expression of molecular markers and cell signals during normal development of the mouse patellar tendon. Tissue Eng Part A 18:598–608. [cited 2014 Oct 10] Available from: http://www.pubmedcentral.nih.gov/articlerender.fcgi?artid=3286855&tool=pmcentrez&rendertype=abstract [PubMed: 21939397]

16. Schwartz a G, Long F, Thomopoulos S. 2015 Enthesis fibrocartilage cells originate from a population of hedgehog responsive cells modulated by the loading environment. Development 142:196–206. [PubMed: 25516975]

17. Zelzer E, Blitz E, Killian ML, et al. 2014 Tendon-to-bone attachment: from development to maturity. Birth Defects Res C Embryo Today 102:101–112. [cited 2014 Oct 20] Available from: http://www.ncbi.nlm.nih.gov/pubmed/24677726 [PubMed: 24677726]

18. Wu Q, Zhang Y, Chen Q. 2001 Indian hedgehog is an essential component of mechanotransduction complex to stimulate chondrocyte proliferation. J Biol Chem 276:35290–35296. [cited 2014 Oct 20] Available from: http://www.ncbi.nlm.nih.gov/pubmed/11466306 [PubMed: 11466306]

19. Ng TC, Chiu KW, Rabie ABHU. 2006 Repeated mechanical loading enhances the expression of Indian hedgehog in condylar cartilage. Front Biosci J Virtual Libr 11:943–948. Available from: http://www.ncbi.nlm.nih.gov/pubmed/16146784

20. Shao YY, Wang L, Welter JF, et al. 2012 Primary cilia modulate Ihh signal transduction in response to hydrostatic loading of growth plate chondrocytes. Bone 50:79–84. [cited 2014 Oct 6] Available from: http://www.pubmedcentral.nih.gov/articlerender.fcgi?artid=3246537&tool=pmcentrez&rendertype=abstract [PubMed: 21930256]

21. Minina E, Wenzel H, Kreschel C. 2001 BMP and Ihh/PTHrP signaling interact to coordinate chondrocyte proliferation and differentiation. Development 128:4523–4534. Available from: http://www.ncbi.nlm.nih.gov/pubmed/?term=BMP+and+Ihh%2FPTHrP+signaling+interact+to+coordinate+chondrocyte+proliferation+and+differentiation [PubMed: 11714677]

22. Mak KK, Kronenberg HM, Chuang P-T, et al. 2008 Indian hedgehog signals independently of PTHrP to promote chondrocyte hypertrophy. Development 135:1947–1956. [cited 2014 Oct 6] Available from: http://www.ncbi.nlm.nih.gov/pubmed/18434416 [PubMed: 18434416]

23. Enomoto-Iwamoto M, Nakamura T, Aikawa T, et al. 2000. Hedgehog proteins stimulate chondrogenic cell differentiation and cartilage formation. J Bone Miner Res 15: 1659–1668.

Available from: http://onlinelibrary.wiley.com/doi/10.1359/jbmr.2000.15.9.1659/abstract [PubMed: 10976986]

24. Vortkamp A, Lee K, Lanske B. 1996 Regulation of rate of cartilage differentiation by Indian hedgehog and PTH-related protein. Science (80-) 273:613–622. [cited 2014 Oct 20] Available from: http://www.sciencemag.org/content/273/5275/613.short
25. Liu C-F, Breidenbach A, Aschbacher-Smith L, et al. 2013 A role for hedgehog signaling in the differentiation of the insertion site of the patellar tendon in the mouse. PLoS ONE 8: e65411 [cited 2014 Oct 20] Available from: http://www.pubmedcentral.nih.gov/articlerender.fcgi?artid=3677907&tool=pmcentrez&rendertype=abstract [PubMed: 23762363]
26. Cohen MM. 2003 The hedgehog signaling network. Am J Med Genet A 123A:5–28. [cited 2014 Nov 2] Available from: http://www.ncbi.nlm.nih.gov/pubmed/14556242 [PubMed: 14556242]
27. Fu S-C, Cheng W-H, Cheuk Y-C, et al. 2013 Effect of graft tensioning on mechanical restoration in a rat model of anterior cruciate ligament reconstruction using free tendon graft. Knee Surg Sports Traumatol Arthrosc 21:1226–1233. [cited 2014 Nov 23] Available from: http://www.ncbi.nlm.nih.gov/pubmed/22461015 [PubMed: 22461015]
28. Thomopoulos S, Genin GM, Galatz LM. 2010 The development and morphogenesis of the tendon-to-bone insertion-What development can teach us about healing. J Musculoskelet Neuronal Interact 10:35–45. Available from: http://www.ncbi. nlm.nih.gov/pmc/articles/PMC3605736/ [PubMed: 20190378]
29. Han X, Guo L, Wang F, et al. 2014 Contribution of PTHrP to mechanical strain-induced fibrochondrogenic differentiation in entheses of Achilles tendon of miniature pigs. J Biomech 47:2406–2414. [cited 2014 Oct 20] Available from: http://www.ncbi.nlm.nih.gov/pubmed/24837216 [PubMed: 24837216]
30. Tang Rabie GH, Hagg ABU. 2004 Indian hedgehog: a mechanotransduction mediator in condylar cartilage. J Dent Res 83:434–438. [PubMed: 15111639]
31. Wu M, Li Y-P, Zhu G, et al. 2014 Chondrocyte-specific knockout of Cbfb reveals the indispensable function of Cbfb in chondrocyte maturation, growth plate development and trabecular bone formation in mice. Int J Biol Sci 10:861–872. [cited 2014 Oct 20] Available from: http://www.pubmedcentral.nih.gov/articlerender.fcgi?artid=4147220&tool=pmcentrez&rendertype=abstract [PubMed: 25170300]
32. Kronenberg HM. 2003 Developmental regulation of the growth plate. Nature 423:332–336. Available from: http://www.ncbi.nlm.nih.gov/pubmed/12748651 [PubMed: 12748651]
33. Studer D, Millan C, Maniura-weber K, et al. 2012 Molecular and biophysical mechanisms regulating hypertrophic 24: 118–135.
34. Kobayashi T, Soegiarto DW, Yang Y, et al. 2005 Indian hedgehog stimulates periarticular chondrocyte differentiation to regulate growth plate length independently of PTHrP 115

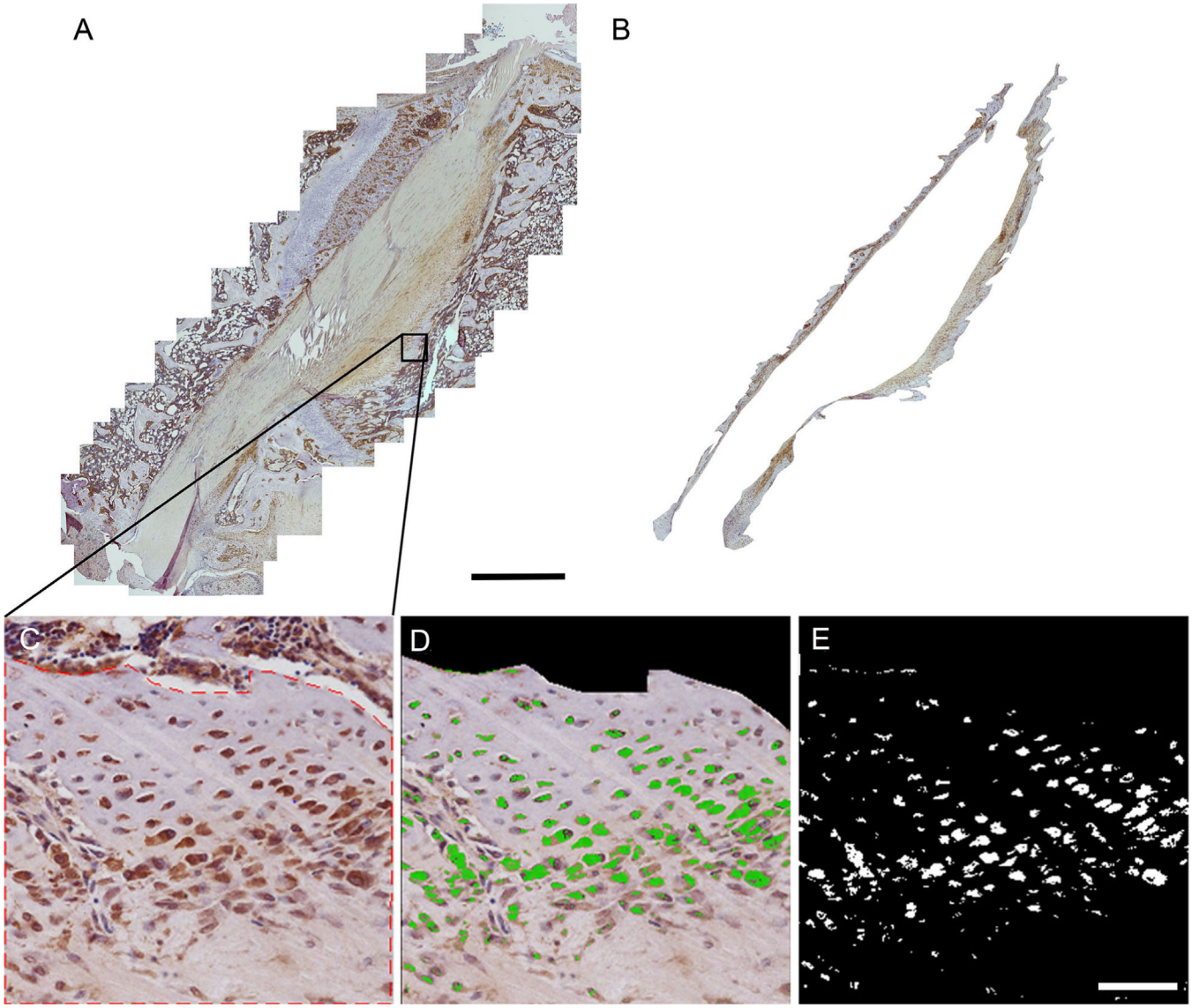

Figure 1.

Image demonstrating quantitative analysis technique. (A) An example of a composite image. Scale bar: 1 mm (B) The same composite image after isolating the tendon-bone interface tissue. (C) Higher magnification image of the tendon-bone interface from selected composite. Red dotted line shows selected area of interest excluding areas of bone marrow. (D) Image demonstrates areas of staining as identified by our computer program. Green areas are considered positive; all other areas are considered negative. Note areas outside designated area of interest which contain positive staining are excluded from computer analysis. (E) Computer generated image in which each pixel considered negatively stained is converted to black while each pixel considered positively stained is converted to white. Scale bar: 100 μm.

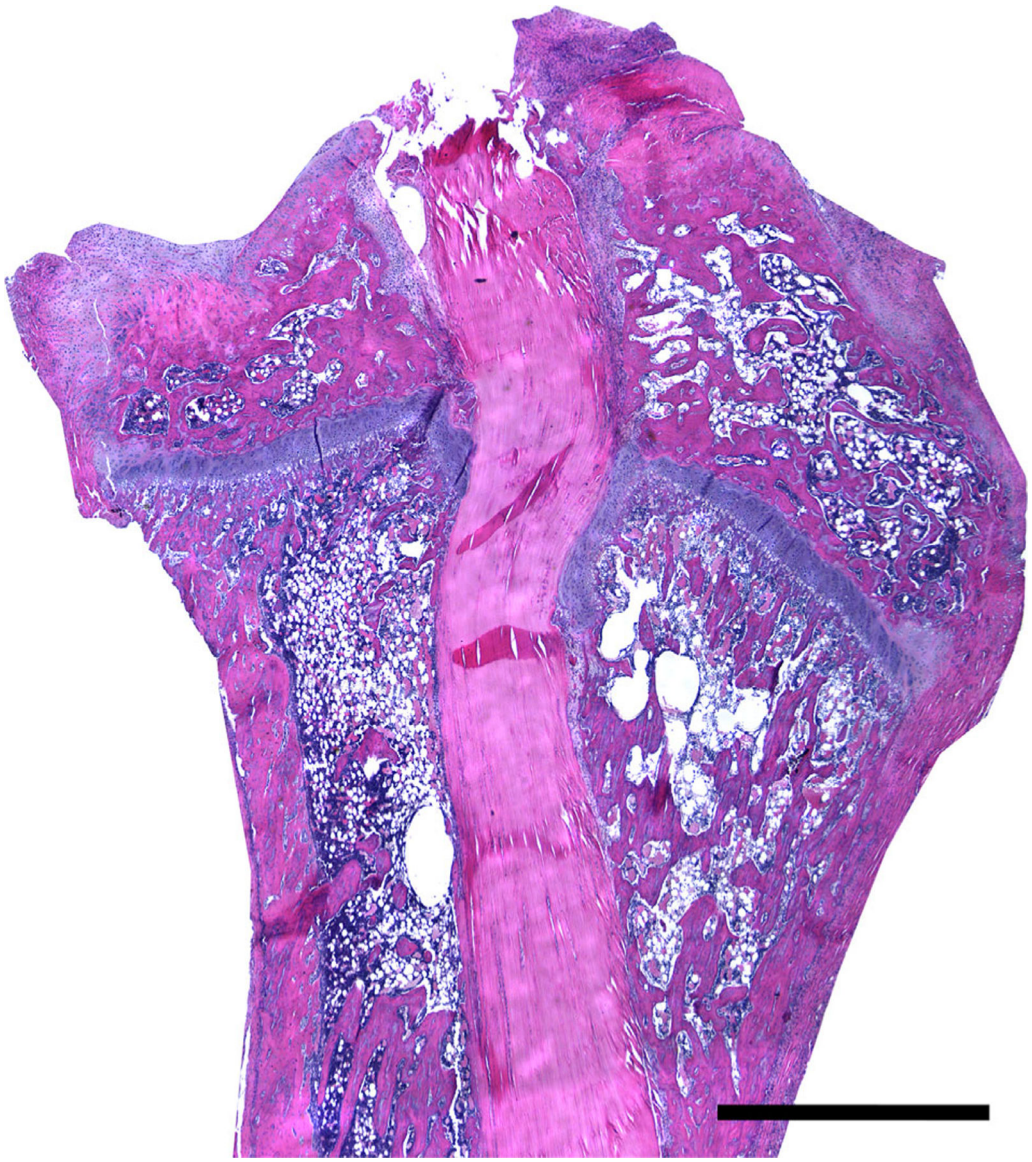

Figure 2.
Low power H&E image showing the entire tendon graft in the tibial tunnel. Scale Bar: 1 mm.

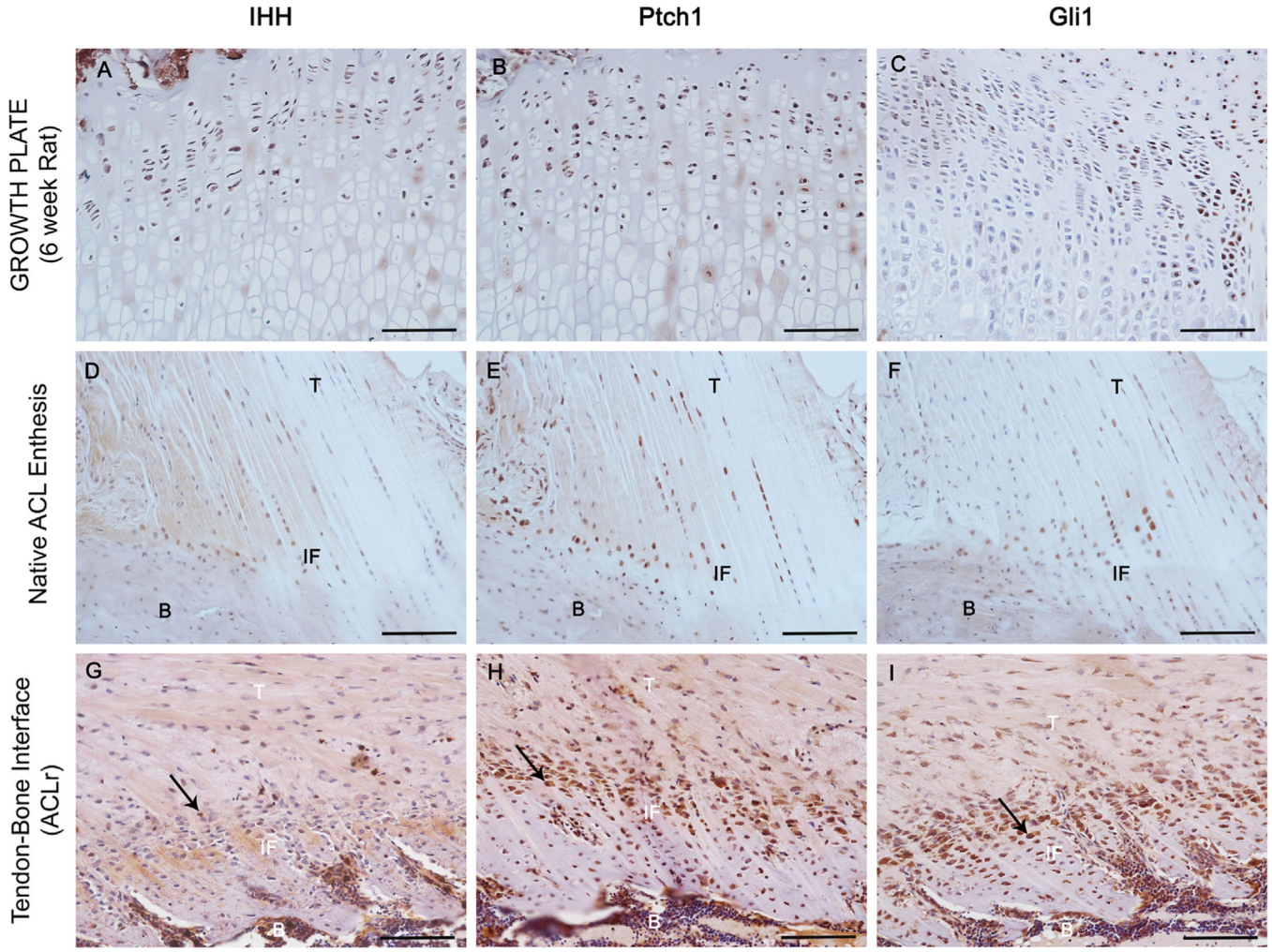

Figure 3.

Immunohistochemical staining for Hh signaling proteins. IHH (A), PTCH (B), and GLI1 (C) staining of a proximal tibial growth plate in a 6 week old rat demonstrating positive Hh signaling. IHH (D), PTCH1 (E), and GLI1 (F) staining of a native ACL enthesis in an age-matched control rat. Representative stains of the tendon-bone interface stained with IHH (H) PTCH1 (I) GLI1 (J) (T, tendon; IF, interface; and B, bone) Arrows identify areas of active staining. Scale bars: 100 μm.

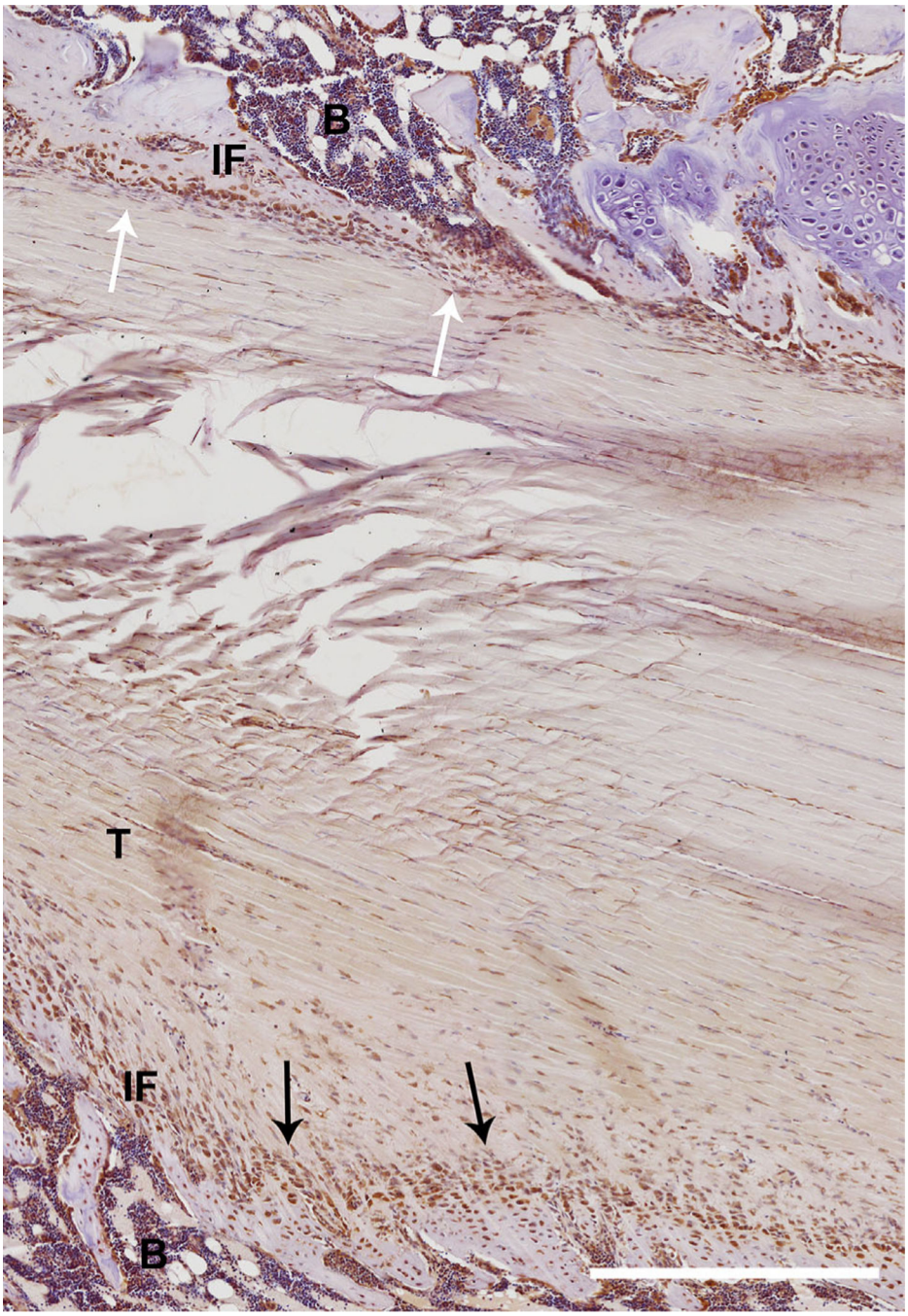

Figure 4.

Low power section stained for GLI1 demonstrating greater tissue organization with alignment of chondrocyte-like cells into columns, as well as a more regular and thicker graft-bone interface (black arrows). On the other side a more irregular and disorganized graft-tendon interface is seen (white arrows). Scale bar: 500 μm.

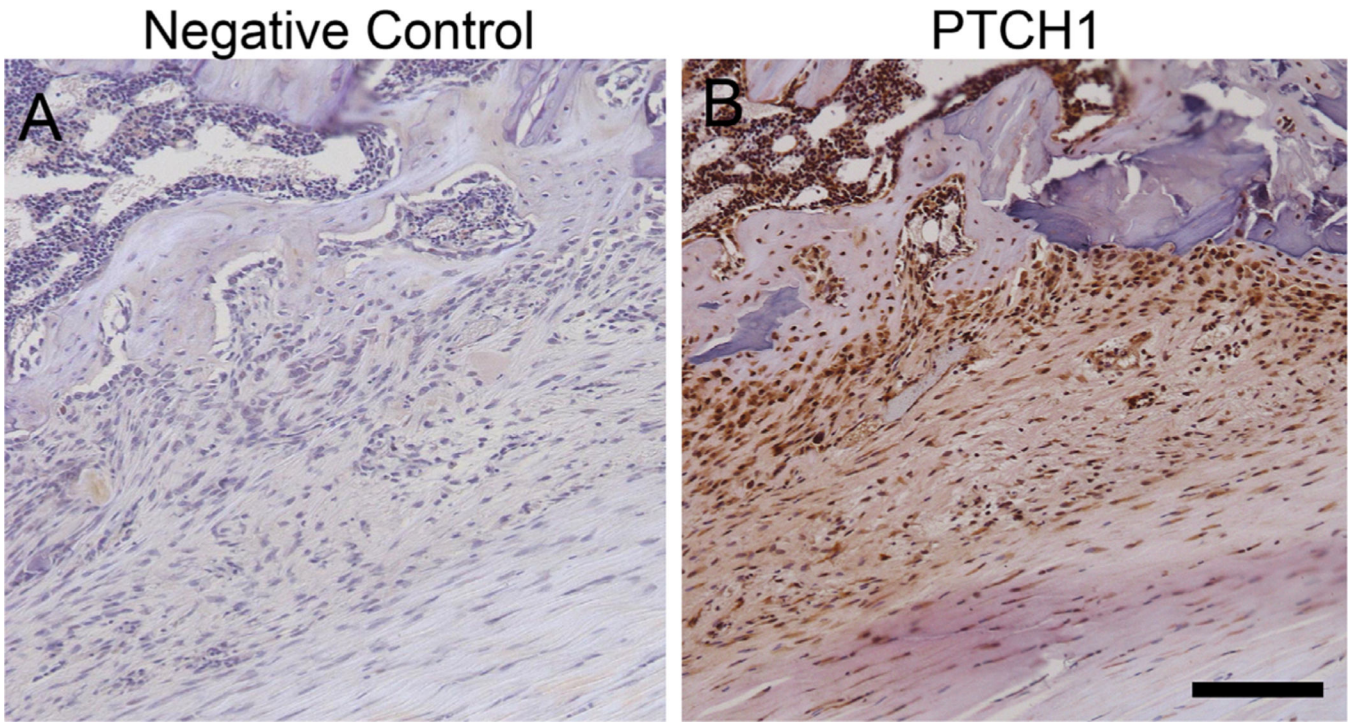

Figure 5.

(A) A representative image of a negative control section demonstrating the absence of staining. (B) A serial section from the same rat in the same region of the tendon bone interface stained with antibody against PTCH1. Scale bar: 100 μm.

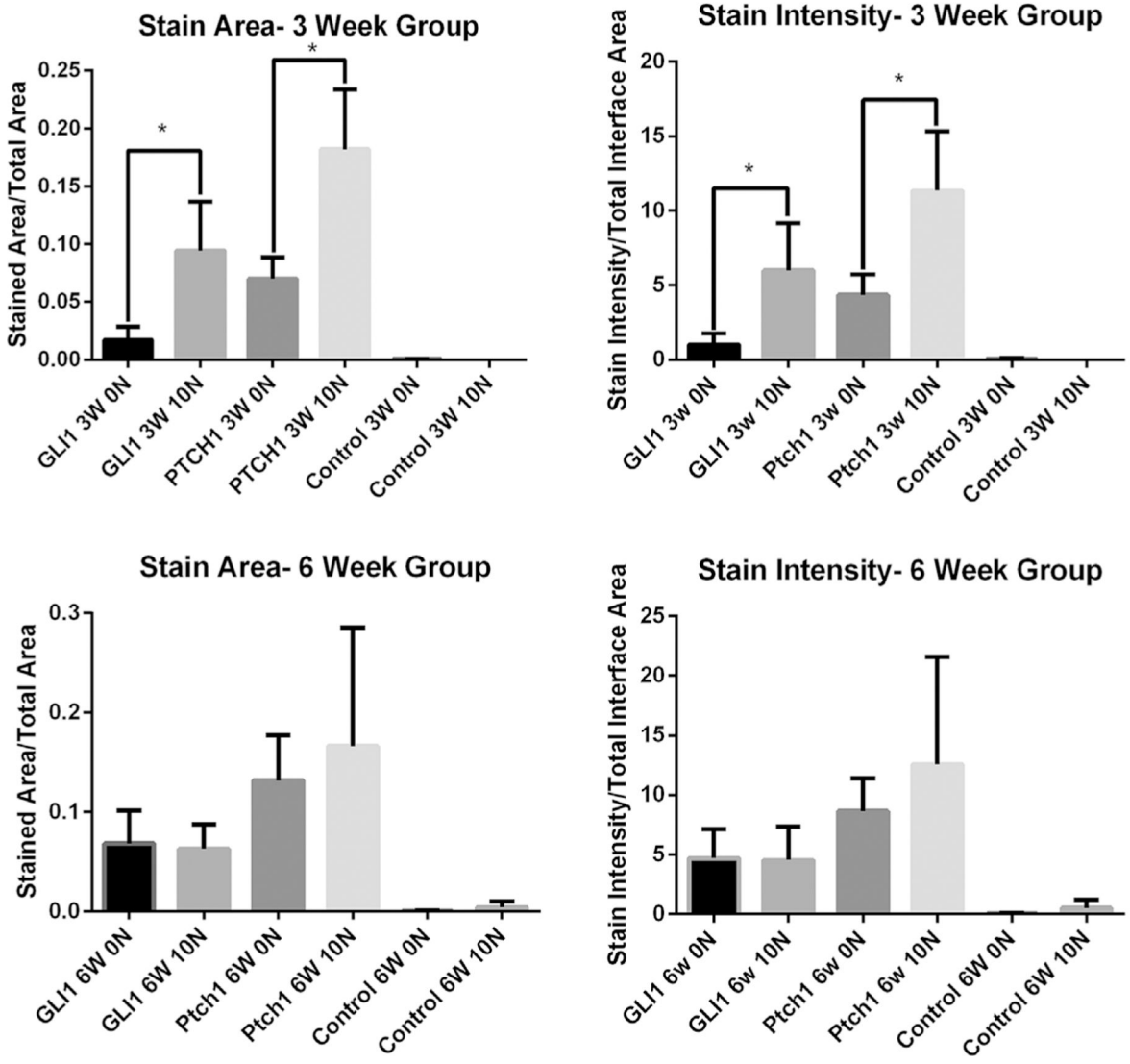

Figure 6.

Quantitative analysis of GLI1 and PTCH1 signaling in terms of both area and intensity of stain at the 3 and 6 week time point. *- denotes *p*-value < 0.05.

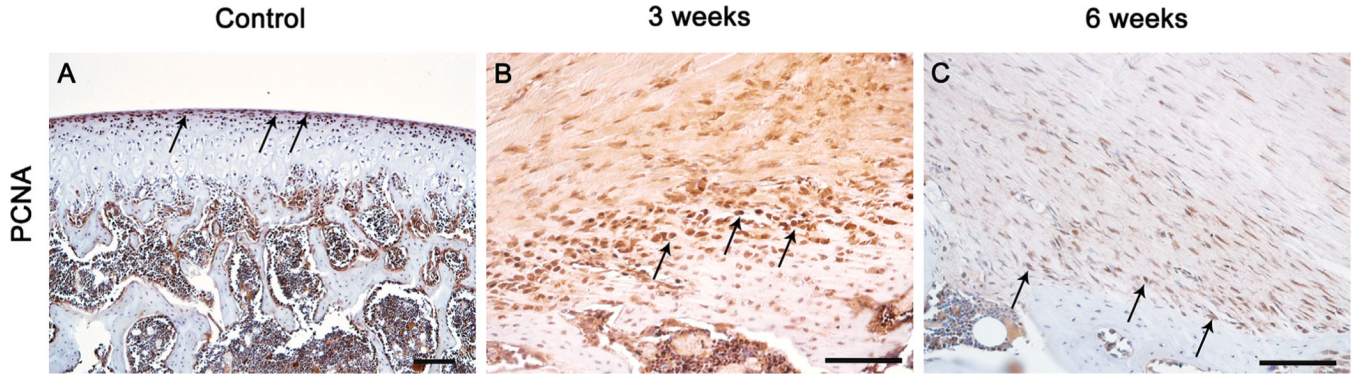

Figure 7.

PCNA staining from the articular cartilage of a 6 week old rat femur which was used as a positive control (A). PCNA staining of the tendon-bone interface 3 (B), and 6 (C) weeks post-ACL reconstruction.

Table 1.

Chart Displaying the Mean Value and Standard Deviation for Each Group

Group	Stained Area/Total Picture Area ± SD	Stain intensity/Total Picture Area ± SD
IHH 3W 0N	0.161±0.143	8.44±4.65
IHH 3W 10N	0.148±0.028	8.95±4.51
IHH 6W 0N	0.122±0.038	7.74±2.89
IHH 6W 10N	0.160±0.078	11.60±6.91
Ptch1 3W 0N	0.070±0.018	4.34±1.40
Ptch1 3W 10N	0.182±0.052	11.34±3.96
Ptch1 6W 0N	0.132±0.045	8.64±2.75
Ptch1 6W 10N	0.166±0.119	12.57±9.00
GLI 3W 0N	0.017±0.011	1.01±0.76
GLI 3W 10N	0.094±0.042	5.99±3.18
GLI 6W 0N	0.068±0.033	4.68±2.45
GLI 6W 10N	0.062±0.025	4.52±2.81
Neg Control 3W 0N	<0.001	0.05±0.06
Neg Control 3W 10N	<0.001	0.01±0.01
Neg Control 6W 0N	<0.001	0.03±0.03
Neg Control 6W 10N	<0.001	0.50±0.70